24th INTERNATIONAL CONGRESS ON SOUND AND VIBRATION
23–27 July 2017, London

ICSV24
23-27JULY 2017
LONDON CALLING

ACOUSTICAL RADIATION PREDICTION FROM SPARSE VIBRATION SAMPLING

Rongfu Mao, Haichao Zhu and Changwei Su

1) Naval University of Engineering, Institute of Noise & Vibration, Wuhan, China

2) National Key Laboratory on Ship Vibration & Noise, Wuhan, China
email: maorfu@163.com

To achieve acoustical radiation prediction from sparse vibration sampling, a method is presented by exploiting of acoustic radiation modes as expansion functions, which are capable of describing geometric shape of vibrating surface. Firstly, acoustic radiation modes of vibrating surface are calculated and the relationship between normal velocity and acoustic radiation modes is built. Then the expressions of normal velocity on actual sparse measurement points by corresponding acoustic radiation mode values are deduced and the amplitude coefficients are determined. Subsequently, all normal velocity values can be reconstructed by the obtained amplitude coefficients and acoustical radiation prediction can be achieved from the reconstructed "sufficient" normal velocities. Experiment validations have been performed on a double-layer steel cylindrical shell with enclosed ends in an anechoic water tank. The theoretic deduction and experiment show that satisfactory results of normal velocity reconstruction and acoustical radiation prediction can be achieved according to the presented method, which demonstrates obvious effectiveness of the presented method.
Keywords: acoustical radiation prediction, sparse vibration sampling, acoustic radiation mode

1. Introduction

In the far-field radiation calculation of vibrating surface, results become more accurate with increasing measurement points [1]. In engineering practice, normal velocity cannot be obtained via analytic methods simply for most vibrating structures, and direct vibration measurement is always adopted. Subsequently, a large number of measurement points are required if accurate far-field results are desired. High measurement cost and heavy load are thus resulted. On the other hand, it's even impossible to arrange sufficient measurement points in some cases such as radiation estimate of large submerged vessels. Therefore, the problem of acoustical radiation prediction from sparse vibration sampling is always arisen to be solved.

There are already some works in the research filed of acoustical radiation prediction from sparse measurement points. In Zhang's work, vibration response of the oil pump was computed by experimental modal expansion technique from several measured points, and then the radiated noise was calculated using BEM method [2]. Although structural modes possess merit of describing geometric shape of vibrating surface, accurate structural modes cannot be obtained conveniently due to the complexity of structures in practice and close dependence on the boundary conditions. Furthermore, structural mode frequencies are often very dense and a lot of locate modes will arise for complicated structures, which always result in the fact that accurate and useful structural modes can hardly be extracted. Wu proposed an interpolation method for the surface velocity of cylindrical

shell structures, in which the surface velocity was expressed by the Fourier series in the circumferential direction and piecewise Lagrange function in the radial direction; smooth velocity distribution could be obtained by the interpolation method from few measured points for further acoustic radiation prediction [3]. Obviously, determined by the principle of the method, its relevant application scope is limited to cylindrical structures. Helmholtz equation least squares (HELS) method was suggested for reconstruction of acoustic radiation by Wang and Wu [4-5], in which the acoustic field was expressed as expansion of a series of spherical harmonic functions. The feature of HELS is low requirement on measurement point number, but it's not suitable for reconstruction of highly non-spherical object surface due to its spherical expansion functions [3].

By summarizing the principles and shortcomings of the mentioned methods, it can be inferred that acoustic radiation prediction task can be fulfilled from sparse measurement points, in case of finding a set of basis functions that can be conveniently obtained and show good geometric shape adaptability to the radiator. Inspired by the inference, an acoustic radiation prediction method from sparse measurement points is presented based on acoustic radiation mode (ARM).

The theory of ARM was put forward in 1990s [6-9]. Based on the ARM theory, all normal velocity on vibrating surface can be expressed by a linear combination of ARMs. In this essence, ARM theory is highly similar to the mentioned structural mode, series expansion and HELS methods with the corresponding expansion functions replaced by ARMs. Due to the features of independence of structural properties and boundary conditions, the calculation of ARMs is much more convenient than that of structural modes. Additionally, compared to other expansion functions, ARMs are capable of describing geometric shape of the vibrating surface. Therefore, the presented ARM based method is expected to fulfil acoustic radiation prediction more appropriately from sparse measurement points.

2. Basic principles

Consider an arbitrary vibrating structure immerged in homogeneous fluid, radiating in free space at frequency ω. If the vibrating surface is discritized into N equal sized elements, the radiated sound power W can be obtained by [9]

$$W = \frac{1}{2}\mathbf{v}_n{}^{\mathrm{H}}\mathbf{R}\mathbf{v}_n, \tag{1}$$

where $\mathbf{v}_n$ is an $N\times 1$ normal velocity vector of vibrating surface, $\mathbf{R}$ represents an $N\times N$ impedance matrix, and superscript "H" denotes Hermitian operator.

Since impedance matrix $\mathbf{R}$ is positive definite and Hermitian, it can be expressed by eigenvalue decomposition as

$$\mathbf{R} = \mathbf{\Phi}^{\mathrm{H}}\mathbf{\Lambda}\mathbf{\Phi}, \tag{2}$$

where $\mathbf{\Lambda}$ is a diagonal matrix with eigenvalues $\lambda_i (i = 1, 2, \cdots N)$ decreasing monotonically along the diagonal, $\mathbf{\Phi}$ represents an $N\times N$ matrix whose columns are eigenvectors $\boldsymbol{\varphi}_i (i = 1, 2, \cdots N)$. Since $\mathbf{R}$ is positive definite and Hermitian, all of its eigenvalues λ_i are positive real and eigenvectors $\boldsymbol{\varphi}_i$ are orthogonal.

From Eq. (2), it can be seen that eigenvectors $\boldsymbol{\varphi}_i$ are a set of basis functions in N dimensional space, and then all arbitrary normal velocity $\mathbf{v}_n$ on the vibrating surface can be expanded uniquely by the eigenvectors $\boldsymbol{\varphi}_i$ as

$$\mathbf{v}_n = \sum_{i=1}^{N} c_i \boldsymbol{\varphi}_i = \boldsymbol{\Phi}\mathbf{c} \quad , \tag{3}$$

where c_i represents amplitude coefficients. As can be seen from Eq. (3), each of eigenvectors $\boldsymbol{\varphi}_i$ represents a particular velocity pattern on vibrating surface, so it's termed as ARM specifically.

In practice, Eq. (3) is always truncated to m $(m < N)$ items for convenience by written as

$$\mathbf{v}_n \approx \sum_{i=1}^{m} c_i \boldsymbol{\varphi}_i = \tilde{\boldsymbol{\Phi}}\tilde{\mathbf{c}}, \tag{4}$$

where $\tilde{\boldsymbol{\Phi}}$ and $\tilde{\mathbf{c}}$ are the first m orders of $\boldsymbol{\Phi}$ and $\mathbf{c}$ respectively.

Suppose the number of measured points on the discritized elements of vibrating surface is l, and normal velocities on the rest of $N-l$ elements remain to be reconstructed. Hence, there are l knowns in the normal velocity vector. Associated equations containing the knowns can be extracted and reorganized into a new equation set as

$$\mathbf{v}'_n \approx \sum_{i=1}^{m} c_i \boldsymbol{\varphi}'_i = \boldsymbol{\Phi}'\tilde{\mathbf{c}}, \tag{5}$$

where $\mathbf{v}'_n$ indicates an vector consisted by the l knowns of $\mathbf{v}_n$, φ'_i represents extracted vector of ARMs corresponding to measurement points in $\mathbf{v}'_n$, and Φ' is composed by m vectors φ'_i. It's worth noting that the extracted vectors φ'_i are not orthogonal any more.

Equation (5) can be solved by singular value decomposition (SVD) if the matrix Φ' is ill conditioned. In general cases, the number of measurement points is greater than the retained number of ARMs, so the coefficient vector $\tilde{\mathbf{c}}$ can be obtained using pseudoinversion

$$\tilde{\mathrm{c}} \approx \left(\Phi'\right)^{+} \mathrm{v}'_n, \tag{6}$$

where superscript "+" denotes pseudoinverse operator, and $\left(\Phi'\right)^{+} = \left[\left(\Phi'\right)^{\mathrm{H}} \Phi'\right]^{-1} \left(\Phi'\right)^{\mathrm{H}}$.

Once the coefficient vector $\tilde{\mathbf{c}}$ is determined, total normal velocity on the vibrating surface can be reconstructed using Eq. (4), and the exact formula is expressed as

$$\mathrm{v}_n \approx \tilde{\Phi}\left(\Phi'\right)^{+} \mathrm{v}'_n. \tag{7}$$

From the obtained "sufficient" normal velocities in Eq. (7), further acoustical radiation prediction can be implemented by all kinds of radiation calculation methods such as BEM, Helmholtz integral formulation and so on. Subsequently, the road of acoustical radiation prediction from sparse measurement points is paved.

It should be noted that Eq. (5) is an inverse problem. In case of improper measurement point arrangement, the condition number of matrix Φ' may be very large. Subsequently, the errors followed with measurement data will be exaggerated and final acoustical prediction may be degraded in severe cases. Therefore, measurement point arrangement should be carefully considered or measurement point optimization methods [10] should be adopted to ensure reasonable condition number of matrix Φ'. Moreover, when noise interference is notable in data measurement, regularization methods can be taken to improve the reconstruction accuracy.

3. Experimental Validation

To examine the validity of the presented method, experiment has been performed on a double-layer steel cylindrical shell with enclosed ends in an anechoic water tank. The length of shell was 2m; the radii of outer layer and inner layer were 0.55m and 0.50m respectively, and corresponding thickness was 0.002m and 0.005m respectively. To suppress additional sound radiation of the two ends, the thickness of two ends was increased to 0.03 m and strengthened by "米" like ribs. Furthermore, the joint space between shell and the ends was sealed by rubber cushion to achieve waterproofness of the shell cabin and attenuation of vibration transmission from the shell body to the ends.

3.1 Experiment setup

The diagram of experiment was shown in Fig. 1. The shell was fixed in an anechoic water tank and a rotor device as the vibration actuators was installed on a foundation structure in the shell. 4(axial direction) × 8(circumferential direction) acceleration transducers were arranged to measure the vibration distribution on the outer layer of the shell, as shown in Fig. 2. A line array constituted by 4 hydrophones was fixed parallel to the shell axis with distance of 5m to measure the sound in the field.

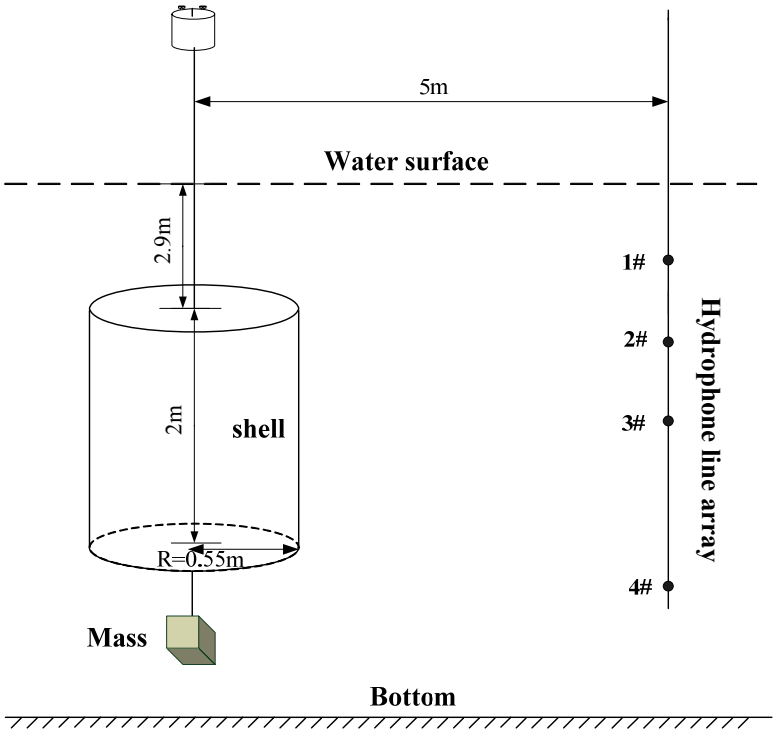

Figure 1: Diagram of the experiment

Data acquisition was done synchronously for all channels after the vibration actuator was stationary. The data sample frequency was 13183Hz, and the time history length of each channel was 20 seconds. Considering reasonable signal noise ratio, the analysis frequency range has been set between 100 and 500 Hz with a resolution of 1 Hz.

After conformation of reasonable condition number of matrix Φ' in Eq.(5), 16 measurement points were picked out from all the 32 measurement points on the outer layer to represent sparse vibration sampling condition. Sound pressure at the hydrophone array was predicted according to the presented method from the picked points, and then the predicted results were compared to actually measured results.

Figure 2: The arrangement of acceleration transducers.

3.2 Analysis and results

The rotor was switched on to excite the cylindrical shell. The excitation energy is mainly centralized at 107 Hz, and typical PSD of acceleration on the outer layer is shown in Fig. 3.

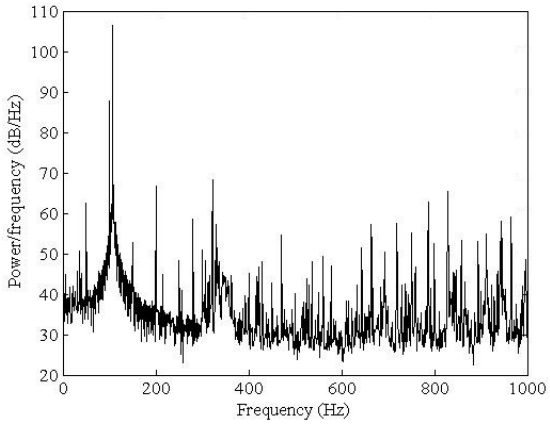

Figure 3: Typical PSD of acceleration on the outer layer for the rotor excitation

At the peak exciting frequency 107 Hz, the measured normal velocity distribution on the outer layer is given in Fig. 4(a), and corresponding "k-space" representation is shown in Fig. 4(b). It can be noted from the figures that associated wavenumber components are distributed not only in the low wavenumber region but also in the high wavenumber area of $kc = \pm 4\text{m}^{-1}$.

As explained above, 16 measurement points were uniformly picked out and corresponding condition number of matrix Φ' is 1.69, which implies reasonable arrangement of the selected sparse measurement points. The selected velocity distribution on the outer layer and corresponding wavenumber distribution are shown in Fig. 5(a) and Fig. 5(b) respectively. It is noted that actual velocity distribution on the outer layer cannot be revealed exactly anymore due to lack of sufficient measurement points, and for "k-space" description, severe loss of vibration related wavenumber components and appearance of additional disturbing components in high wavenumber region are also observed evidently.

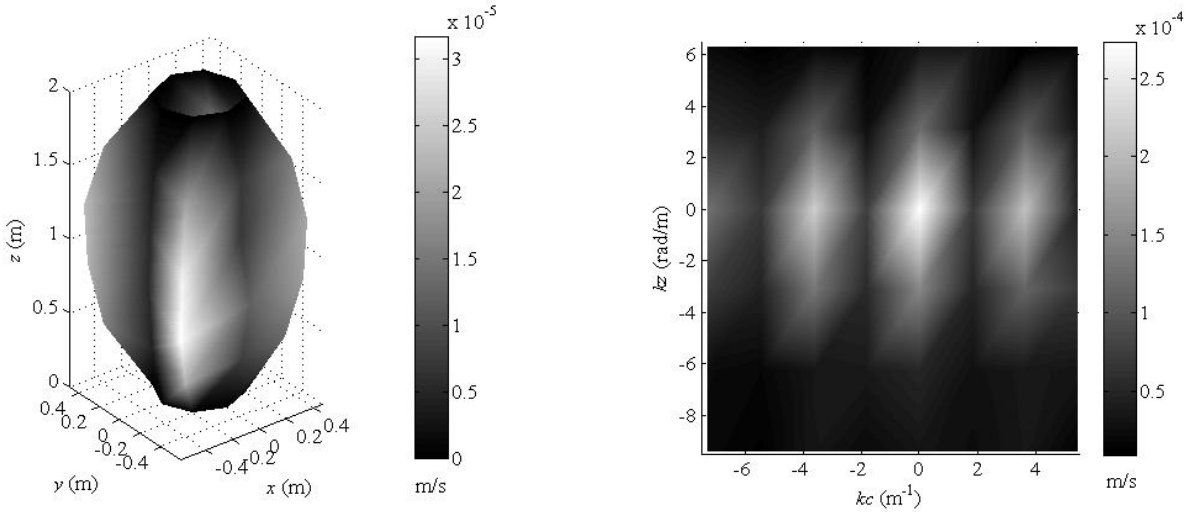

(a) (b)

Figure 4: Measured normal velocity and "k-space" distribution. (a) Measured normal velocity distribution; (b) "k-space" distribution.

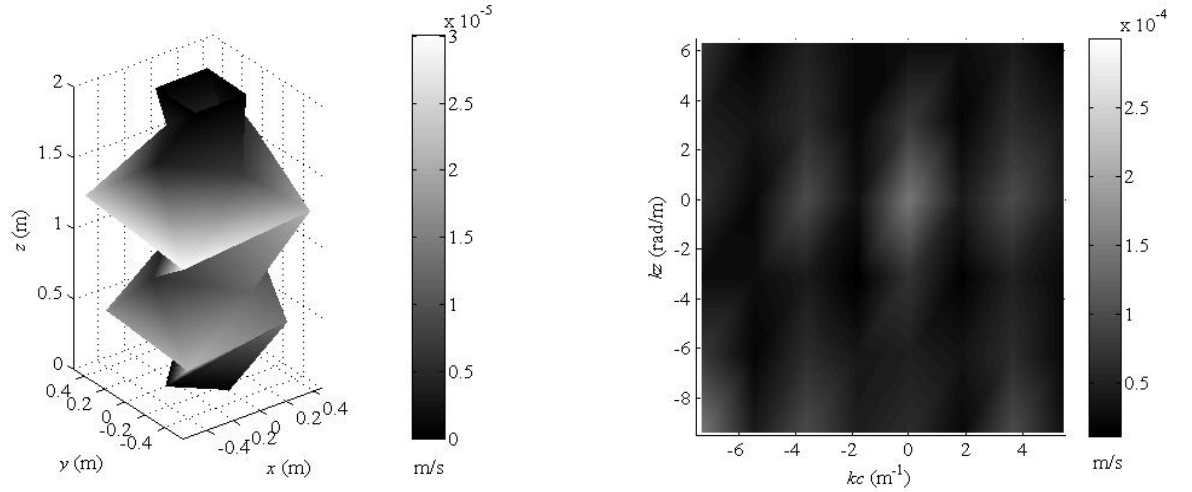

(a) (b)

Figure 5: Selected normal velocity and "k-space" distribution. (a) Selected normal velocity distribution; (b) "k-space" distribution.

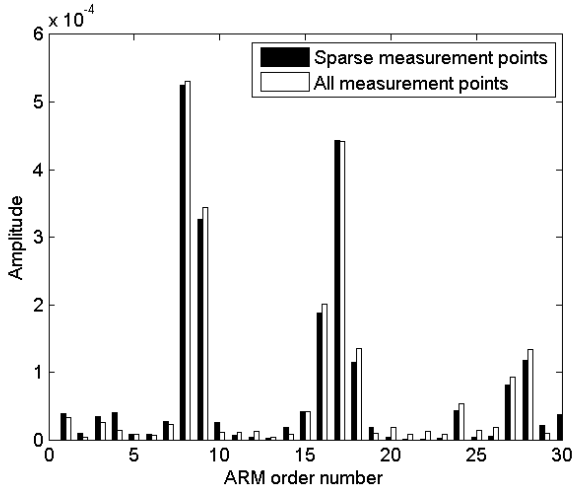

Figure 6: Amplitude coefficient results from sparse measurement points and all measurement points

According to the presented method, amplitude coefficient can be calculated from the selected sparse measurement points, which is depicted in Fig. 6. In order to inspect the accuracy of the presented method, amplitude coefficient result calculated from all measurement points is also given in Fig. 6. As can be seen, results from above two dataset coincide very well, which ensures the accuracy of normal velocity reconstruction and final acoustic radiation prediction from sparse vibration sampling.

Next, total normal velocity can be reconstructed from the picked sparse measurement points. Considering both amplitude coefficient in Fig.6 and fast decay of radiation efficiency with growing ARM orders, first 30 ARMs are truncated in the calculation. The relative error between the reconstructed results and actually measured data is about 10.3%. Figure 7 (a) and Fig.7 (b) illustrate the reconstructed normal velocity distribution and the corresponding "k-space" distribution respectively. Compared the results to Figs. 4 (a) and 4 (b), it is clearly demonstrated that both normal velocity and corresponding wavenumber components can be restored accurately.

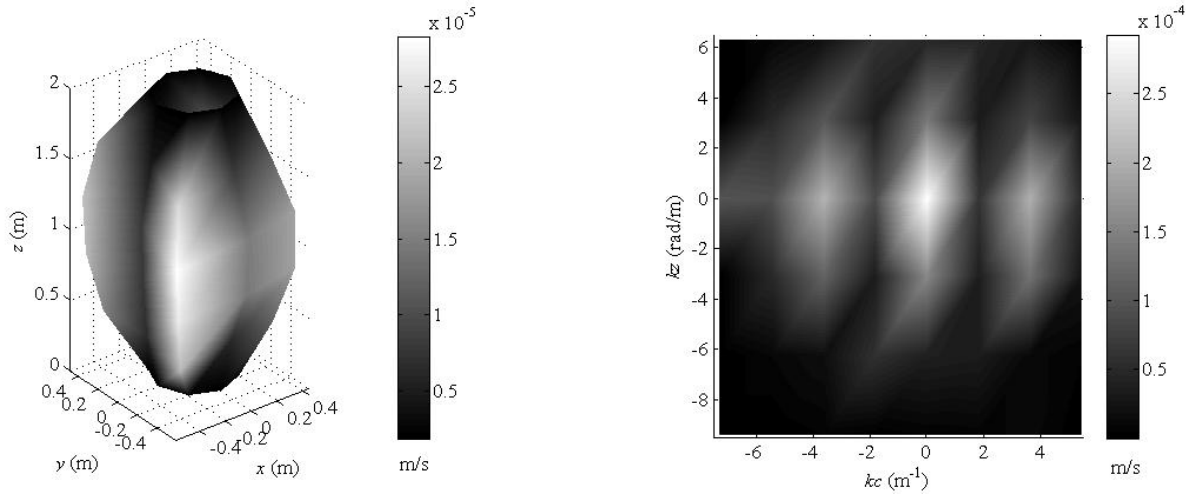

(a) (b)

Figure 7: Reconstructed normal velocity and "k-space" distribution. (a) Reconstructed normal velocity; (b) "k-space" distribution.

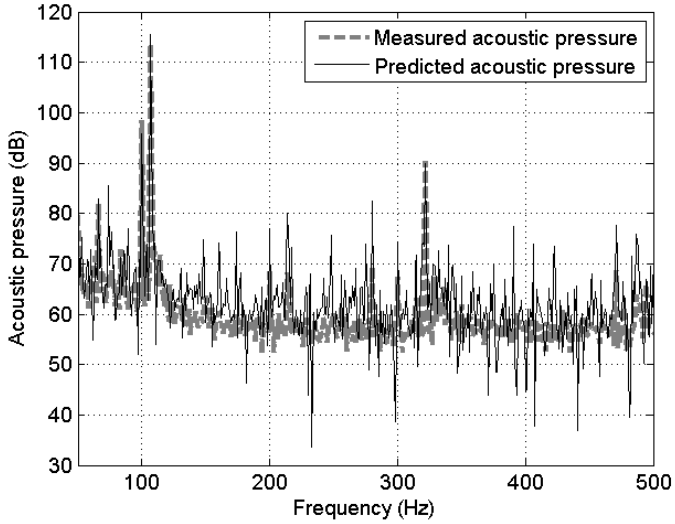

Figure 8: Comparison of predicted pressure and measured pressure of 1# hydrophone (ref=10^{-6}Pa)

Finally, from the reconstructed "sufficient" normal velocities, acoustic pressure at the hydrophone array can be predicted by Helmholtz integral formulation. Predicted pressure and actually measured pressure of 1# hydrophone in 50~500 Hz frequency band are compared in Fig. 8. As can be seen, at the good SNR frequencies like exciting frequency 107 Hz, the predicted result from sparse sampling coincide with the measured signal very well, which demonstrates obvious effectiveness of the presented method. The results of the other three hydrophones are almost the same and omitted for concision.

4. Conclusions

To achieve acoustical radiation prediction from sparse vibration sampling, a method is presented by utilization of ARMs as expansion functions and experiment validations have been performed. From the theoretic deduction and experiment results, some conclusions can be drawn as follows:

(1) Actual velocity distribution cannot be revealed exactly with sparse measurement points, which corresponding to severe loss of vibration related wavenumber components and appearance of additional disturbing components in high wavenumber region.

(2) The theoretic deduction and experiment show that satisfactory results of normal velocity reconstruction and acoustical radiation prediction from sparse vibration sampling can be achieved according to the presented method.

Acknowledgements

The authors would like to thank Dr. Liang Guo and Junbo Su for their assistance in the experiment implementation. The work is supported by the National Natural Science Foundation of China, Grant No. 51305452.

REFERENCES

1 Tao J., Ge H., and Qiu X. A new rule of vibration sampling for predicting acoustical radiation from rectangular plates, *Applied Acoustics*, 67(8): 756-770, (2006).

2 Zhang J.H., Liu Y.H.,and Wang J.S. Study on radiated noise of engine oil sump by experimental modal expansion technique, *Transactions of CSICE,* 23(6), 532-535, (2005). (in Chinese)

3 H.J. Wu, Y.L. Zhang, W.K. Jiang, An interpolation method for the measured velocity and its application in the prediction of acoustic radiation of submerged cylindrical shell structures, *ACTA ACUSTICA*, 40(5), 631-638, (2015). (In Chinese)

4 Wang Z.X., Wu S.F. Helmholtz equation–least-squares method for reconstructing the acoustic pressure field, *J. Acoust. Soc. Am,* 102(4), 2020-2032,(1997).

5 Zhao X., Wu S.F. Reconstruction of vibro-acoustic fields using hybrid nearfield acoustic holography, *J. Sound Vib.*, 282: 1183–1199, (2005).

6 Borgiotti G.V. The power radiated by a vibrating body in an acoustic fluid and its determination from boundary measurements, *J. Acoust. Soc. Am,* 88(4), 1884–1893,(1990).

7 Elliott S.J., Johnson M.E. Radiation modes and the active control of sound power, *J. Acoust. Soc. Am,* 94(4), 2194–2204, (1993).

8 Borgiotti G.V., Jones K.E. The determination of the acoustic farfield of a radiating body in an acoustic fluid from boundary measurements, *J. Acoust. Soc. Am,* 93(5), 2788–2797, (1993).

9 Gary P.G., Robert L.C., et al. Radiation modal expansion: Application to active structural acoustic control, *J. Acoust. Soc. Am,* 107(1), 332-339, (2000).

10 Zhang Z., Nickolas V. A computational acoustic field reconstruction process based on an indirect boundary element formulation, *J. Acoust. Soc. Am,* 108(5 Pt 1), 2167-2178, (2000).